Ocean Dynamics (2014) 64:1025–1038
DOI 10.1007/s10236-014-0737-2

A method for finding the optimal predictor indices for local wave climate conditions

Paula Camus · Fernando J. Méndez · Inigo J. Losada · Melisa Menéndez · Antonio Espejo · Jorge Pérez · Ana Rueda · Yanira Guanche

Received: 22 January 2014 / Accepted: 21 May 2014 / Published online: 10 June 2014

Abstract In this study, a method to obtain local wave predictor indices that take into account the wave generation process is described and applied to several locations. The method is based on a statistical model that relates significant wave height with an atmospheric predictor, defined by sea level pressure fields. The predictor is composed of a local and a regional part, representing the sea and the swell wave components, respectively. The spatial domain of the predictor is determined using the Evaluation of Source and Travel-time of wave Energy reaching a Local Area (ESTELA) method. The regional component of the predictor includes the recent historical atmospheric conditions responsible for the swell wave component at the target point. The regional predictor component has a historical temporal coverage (*n*-days) different to the local predictor component (daily coverage). Principal component analysis is applied to the daily predictor in order to detect the dominant variability patterns and their temporal coefficients. Multivariate regression model, fitted at daily scale for different *n*-days of the regional predictor, determines the optimum historical coverage. The monthly wave predictor indices are selected applying a regression model using the monthly values of the principal components of the daily predictor, with the optimum temporal coverage for the regional predictor. The daily predictor can be used in wave climate projections, while the monthly predictor can help to understand wave climate variability or long-term coastal morphodynamic anomalies.

Keywords Wave climate indices · Wave climate variability · Multivariate regression · Statistical downscaling

Responsible Editor: Oyvind Breivik

This article is part of the Topical Collection on the *13th International Workshop on Wave Hindcasting and Forecasting in Banff, Alberta, Canada October 27 - November 1, 2013*

P. Camus (✉) · F. J. Méndez · I. J. Losada · M. Menéndez · A. Espejo · J. Pérez · A. Rueda · Y. Guanche
Environmental Hydraulics Institute "IH Cantabria", Universidad de Cantabria, C/Isabel Torres nº 15. Parque Científico y Tecnológico, 39011 Santander, Spain
e-mail: camusp@unican.es

1 Introduction

Atmospheric climate variability can be explained by principal circulation modes and the temporal variation of these modes is usually defined as a climate index. The North Atlantic Oscillation (NAO) was the first regional signal identified (Walker and Bliss 1932), with the corresponding index being defined, e.g., as the normalized pressure difference between Iceland and Portugal (Hurrell 1995). The Southern Oscillation Index (SOI) is another principal large-scale fluctuation in air pressure occurring between the western and eastern tropical Pacific during El Niño and La Niña episodes. This index is calculated based on the normalized air pressure differences between Tahiti and Darwin, Australia (Ropelewski and Jones 1987). Other important climate indices are the North Pacific Index (NPI, Trenberth and Hurrell 1994), which represents the strength of the northeastern Pacific westerlies; the Arctic Oscillation (AO), a hemispheric phenomenon characterized by a semi-permanent low pressure over the North Pole (Thompson and Wallace 1998); the Antarctic Oscillation (AAO), also known as the Southern Annular Mode (SAM), a similar variability pattern to the AO in the Southern Hemisphere (Thompson and Wallace 1998). These climate indices can be obtained applying principal component analysis (PCA) to atmospheric variables, mainly pressure fields.

Interannual variability of wave climate has been explored using these well-known climate indices. The correlation between waves and climate indices has been analyzed using different databases (e.g., global wave reanalysis as C-ERA-

40, Sterl and Caires 2005; visual data, Gulev and Grigorieva 2006; altimeter data, Woolf et al. 2002) or separating the sea and swell component (Semedo et al. 2011; Gulev and Grigorieva 2006). The analysis has also been performed calculating spatial correlation patterns (Stopa et al. 2012; Fan et al. 2012; Dodet et al. 2010; Hemer et al. 2010) or correlating the first principal components of wave fields obtained from PCA (Sterl and Caires 2005; Gulev and Grigorieva 2006; Semedo et al. 2011). These indices have been used also to estimate the interannual variability of extreme waves, included as covariates in a time-dependent extreme distribution (e.g., Izaguirre et al. (2010) and Izaguirre et al. (2011), using wave altimeter data; Hemer 2010, using buoy data).

The interannual variability has also been modeled using covariates defined as the seasonal mean sea level pressure (SLP) anomalies and the squared SLP gradient index, calculated in a local area enclosing the target point (Wang et al. 2004; Wang and Swail 2006; Caires et al. 2006). Seasonal mean SLP fields over a regional area (e.g., North Atlantic or North Pacific) have also been used as a predictor in statistical models that simulate seasonal mean or 90th percentiles of significant wave height (Wang et al. 2004). Besides, due to the fact that every sea state at a particular location is usually a mix of sea and swell components, a local predictor and a regional predictor are used to simulate the sea and swell wave components at an hourly scale, respectively (Wang et al. 2012; Casas-Prat et al. 2014).

The well-known climate indices explain the atmospheric variability at certain large regions. However, waves are generated by a combination of local and remote winds, being required two predictor components with not only different spatial domain but also different temporal ranges. Thus, there is a need for developing specific wave predictor indices for evaluating wave climate variability at a specific location.

Some considerations about atmospheric conditions must be taken into account in order to find temporal coefficients of atmospheric variability modes as possible wave predictor indices. The surface wind field is the main force of wave heights. However, in global circulation models, sea wind fields are not as well reproduced as sea level pressure fields (Caires et al. 2006). Besides, the geostrophic wind direction is well-represented by the isobars, and geostrophic wind speed is proportional to the pressure gradient. The SLP fields and the square SLP gradients are, therefore, considered to define the wave predictor indices, in line with the downscaling statistical predictor used by Wang et al. (2012) and Casas-Prat et al. (2014). Moreover, two components, with different spatial extensions and different historical temporal coverages, are used in order to characterize sea and swell components of the wave climate. The ESTELA method (Evaluation of Source and Travel-time of wave Energy reaching a Local Area, Perez et al. 2014, in this volume) is applied to define the spatial domains and the temporal ranges of the atmospheric fields. The variability patterns are identified by applying a statistical model that relates the local significant wave height with the atmospheric conditions at daily and monthly scale.

The aim of this work is to present a method for obtaining useful predictor indices to characterize wave climate at any location worldwide. The developed semi-automatic method improves the spatial and temporal definitions of the predictor components and provides additional information of wave climate variability. The rest of the article is structured as follows: the method proposed to define the wave predictor indices is described in Section 2. The steps of the method are explained in detail by means of an application in Section 3. Other examples of wave predictor indices at locations with different wave climatology are presented in Section 4. Section 5 completes the study with a summary and some concluding remarks.

2 Method

A flowchart of the method proposed to define local wave predictor indices is shown in Fig. 1. Both simultaneous historical sea level pressure fields (predictor) and significant wave height (predictand) databases are required as inputs. This information is usually available from reanalysis databases at 6-hourly resolution.

The predictor is defined by a local component which represents the sea wave component and a regional one which represents the swell wave component. The different spatial domain and historical temporal range of both predictor components have to be defined according to the local wave climate at the target location. The ESTELA method (Perez et al. 2014) is applied to define these two relevant factors. Local predictor reproduces waves reaching to the target location within 1 day. Regional predictor covers a geographic area of all possible waves reaching the target location with a historical temporal coverage (the same day as the local predictor and several previous days). These n-days should capture the recent atmospheric conditions responsible of the swell wave component. Therefore, the predictor is defined at a daily scale joining the daily mean SLP in the local spatial domain and the n-days means in the regional domain. The principal component analysis (PCA) is then applied to the daily predictor fields in order to obtain the dominant spatial variability patterns and their corresponding temporal coefficients.

Regarding the predictand, the daily mean significant wave height is processed from the input wave reanalysis. For each n-days, a multivariate regression model is fitted between daily significant wave height and principal components of the daily predictor. The n-days associated to the best multivariate regression model fit is chosen to be the optimal historical temporal coverage of the regional predictor.

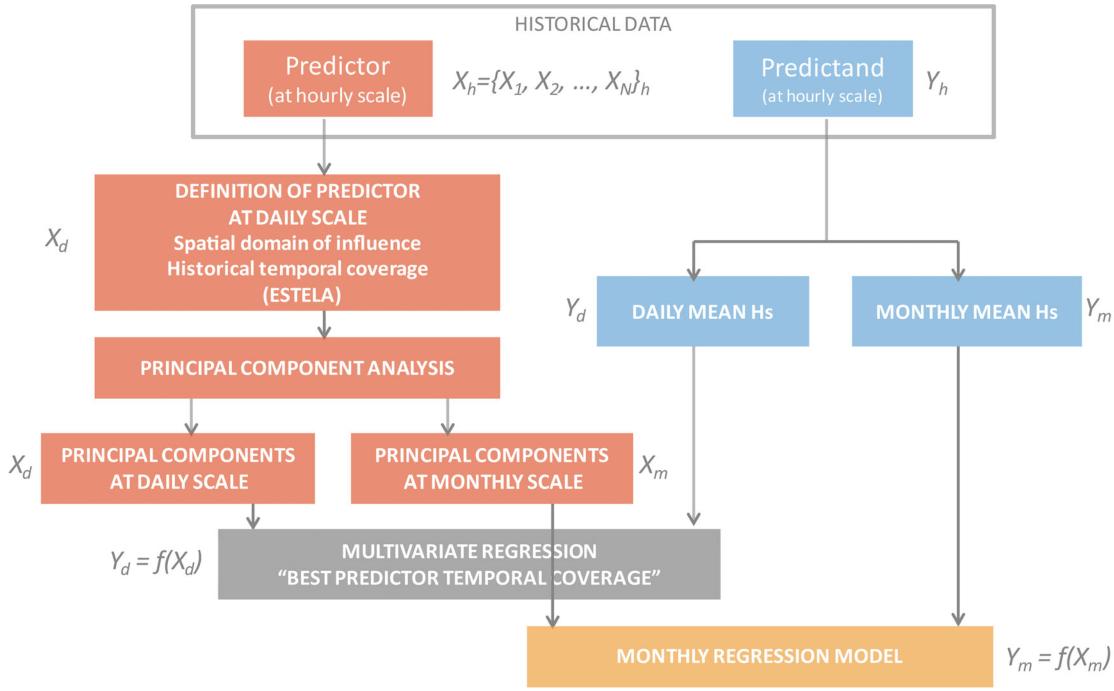

Fig. 1 Flow chart to obtain predictor indices for wave conditions

Monthly wave predictor indices for a target location are selected, applying a multivariate regression model between the local monthly significant wave height and monthly values of the principal components of the daily predictor with the optimum historical temporal coverage of the regional predictor.

3 Application

In this section, we describe the steps of the method in more detail through applying it on a particular location in the northwest coast of Spain.

3.1 Data

The atmospheric data used in this work as the predictor come from the reanalysis dataset of the National Center for Environmental Prediction-National Center for Atmospheric Research (NCEP/NCAR, Kalnay et al. 1996). The historical wave data used as predictand is the Global Ocean Wave reanalysis (GOW, Reguero et al. 2012). Both data sets comprise a common period of time of 60 years, from 1948 to 2008.

The NCEP/NCAR reanalysis SLP data consist of 6-hourly fields on a Gaussian grid with T62 resolution (about 210 km). The GOW database is an up-to-date wave dataset with global coverage and hourly resolution. The global wave dataset has a grid with a spatial resolution of 1.5° in longitude and 1° in latitude and was computed using the model WAVEWATCH III (Tolman 2002) forced with 6-hourly wind fields from the NCEP/NCAR reanalysis project. Bathymetry data used for the simulation comes from the ETOPO dataset (NOAA 2006). A post-process using altimetry data has been applied consisting of (a) the identification of possible outliers due to tropical cyclones not correctly simulated because of insufficient resolution in the wind forcing (Mínguez et al. 2012) and (b) a directional correction procedure (Mínguez et al. 2011) of the simulated significant wave heights, especially remarkable for large values of wave height. The database has been compared with other existing global analysis showing similar quality with the advantage of providing longer time records.

3.2 Spatial predictor definition

The ESTELA method (Perez et al. 2014, in this issue) is applied to define the predictor area of influence and the possible historical temporal coverage of the regional predictor component.

The ESTELA method provides the effective energy flux in a spatial domain and the wave travel time for the target location. The method is based on wave hindcast data using both geographic-based and physically based criteria. Geographic criterion is applied to limit the study into the relevant spatial domain. The valid source points in the selected spatial domain are linked to the target location along a great circle path without any interruption. Frequency-direction wave information from a global wave parameter database (Rascle et al. 2008; Rascle and Ardhuin 2012) is used to calculate the energy flux at each source point. The wave spectra have been reconstructed using the significant wave

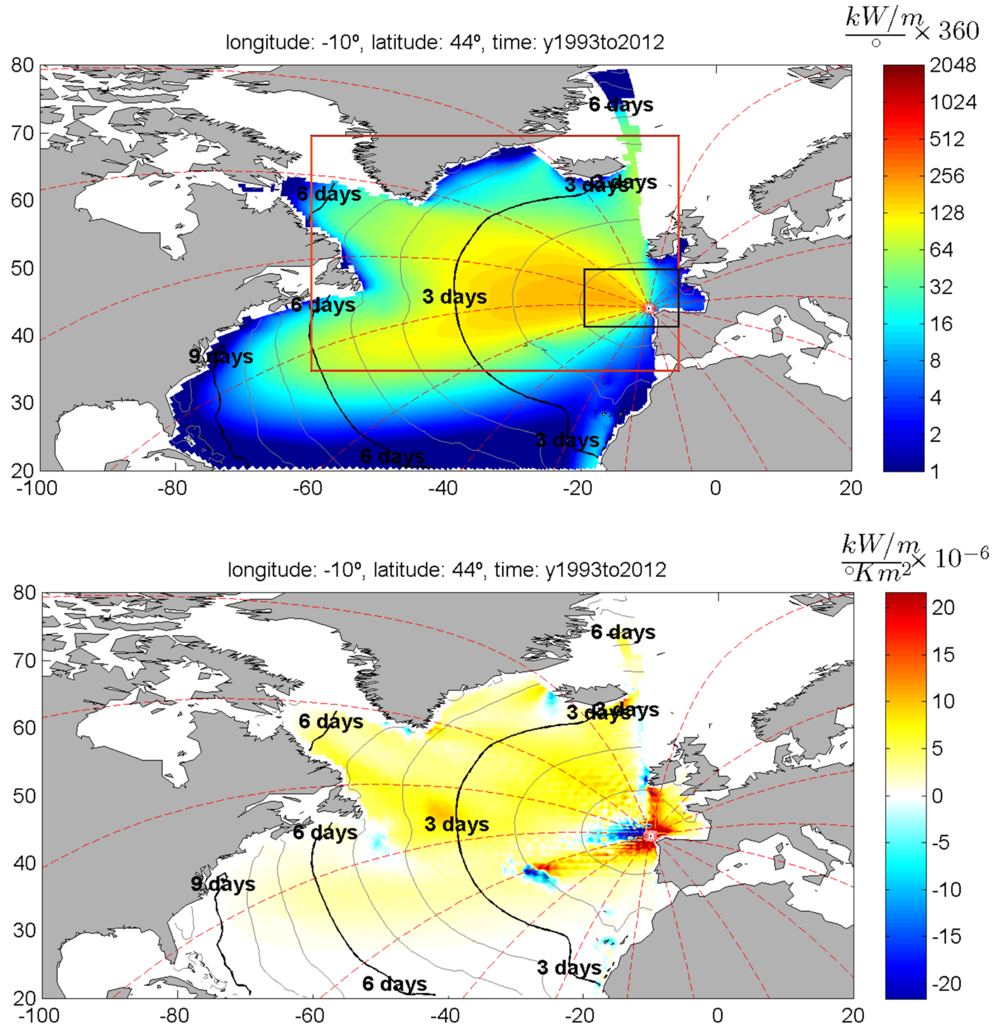

Fig. 2 Effective energy flux at the source points for the target point at the Spanish northwest coast (*upper panel*). Travel time in days is represented by the *gray* and *black lines*. *Red dashed lines* represent great circles for 16 directional sectors. The *red* and *black boxes* are the spatial domain of the regional predictor and the local predictor, respectively. Gain/loss of energy flux for the target point at the Spanish northwest location (*lower panel*)

height, peak period, mean direction, and directional spread for up to six partitions of the spectrum, the wind sea, and five swell trains in the more general case. This information is provided in a spatial grid at 0.5° resolution and 3-hourly time resolution from 1993 to 2012. The effective energy flux for all the source points is calculated taking into account only the energy traveling towards the target point of each 3-hourly wave spectrum (physical criterion), at the group velocity, removing the amount of energy loss by viscous dissipation. The gain/loss of energy in each cell can be viewed as the difference between the incoming and the outcoming flux along the great circle. The analysis of ESTELA maps for specific time periods can be used to analyze the wave climate variability. In this application, the mean effective energy flux is considered to identify the spatial domain of influence for wave generation at a specific location. The predictor area for statistical downscaling is established almost automatically.

The upper panel of Fig. 2 represents the effective energy flux at the source points for the selected location in the northwest Spanish coast [10° W, 44° N], from the lowest energy (blue color) to the largest energy (red). Red dashed lines represent great circles for 16 directional sectors. Gray and black lines represent the wave energy travel time, in days. The lower panel represents the gain/loss of energy flux, informing about important wind-seas in a local area around the target point and 2–6 days swells from the whole North Atlantic Ocean. In this case, it can be observed that wave energy is generated and comes from a large area extended over the North Atlantic Ocean. The areas of energy loss could be explained by (1) wind-seas forcing waves to propagate in directions away from the target point, increasing directional spread and (2) the uncertainties associated to the spectra

Fig. 3 The first six empirical orthogonal functions (EOFs) and principal components (PCs) of the predictor defined to obtain the monthly wave climate indices at a given location at the Spanish northwest coast. The SLP anomalies are represented by *contour lines*, plotting the positive anomalies in *red* and the negative in *blue*. The anomalies of the squared SLP gradients are represented in a *blue-white-red* scale

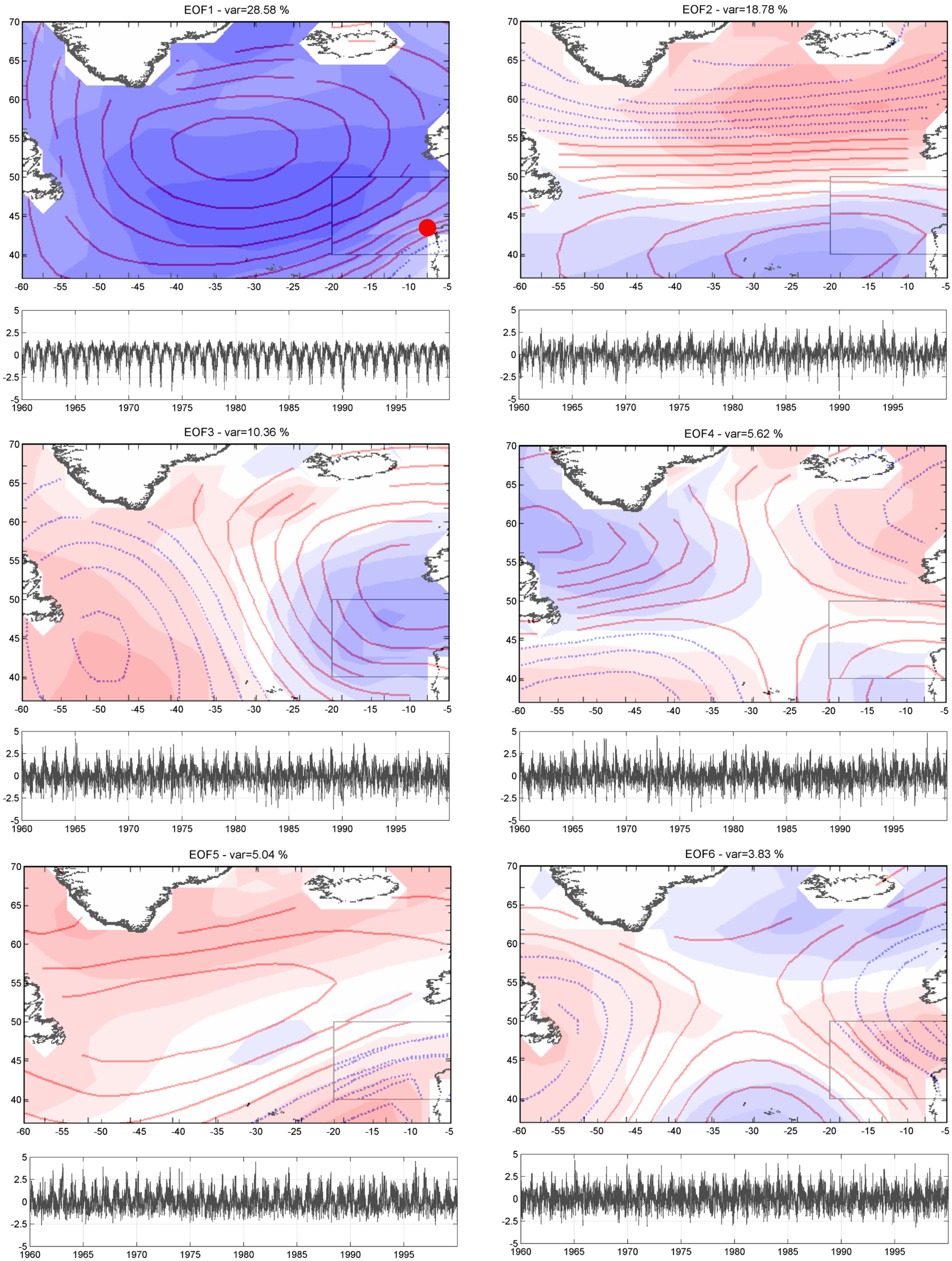
EOF1 - var=28.58 %
EOF2 - var=18.78 %
EOF3 - var=10.36 %
EOF4 - var=5.62 %
EOF5 - var=5.04 %
EOF6 - var=3.83 %
70 65 60 55 50 45 40
-60 -55 -50 -45 -40 -35 -30 -25 -20 -15 -10 -5
5 2.5 0 -2.5 -5
1960 1965 1970 1975 1980 1985 1990 1995

reconstruction for those grid points with the highest incoming energy close to the target location.

Based on the ESTELA results, the spatial domain of the predictor for the swell wave component is defined as an area of the North Atlantic Ocean, spanning from 35° N to 70° N and from 60° W to 5° W, with a 2.5° spatial resolution (regional area). The predictor for the sea component is defined as a smaller area limited by the 1-day travel time region, spanning from 40° N to 50° N and from 20° W to 5° W (local area).

The method requires the definition of a historical temporal coverage in the regional spatial domain. The temporal coverage of the predictor is established as the *n*-days in the regional area (from 2 to 9 days) and 1 day in the local area, using the averaged SLP and the averaged squared SLP gradients with the corresponding temporal coverage. The daily predictor is calculated as the daily mean fields in the local area and the *n*-days mean fields in the regional area, being the last day of the *n*-days temporal coverage of the regional predictor component coincident with the day of the local predictor component.

PCA is a statistical technique widely used in climatology to identify dominant variability patterns and reduce dimensionality. PCA is applied to the daily predictor to detect the main variability modes of the wave predictor for the target location considered and the temporal coefficients of the identified patterns. PCA projects the original data on a new space, searching for the maximum variance of the sample data. The eigenvectors (empirical orthogonal functions, EOFs) of the data covariance matrix define the vectors of the new space. The transformed components of the original data over the new vectors are the principal components (PCs). The original predictor *X(x,t)* can be expressed as a linear combination of EOFs and PCs:

$$X(x,t_i) = EOF_1(x) \times PC_1(t_i) + EOF_2(x) \times PC_2(t_i) + \ldots \quad (1)$$
$$+ EOF_N(x) \times PC_N(t_i)$$

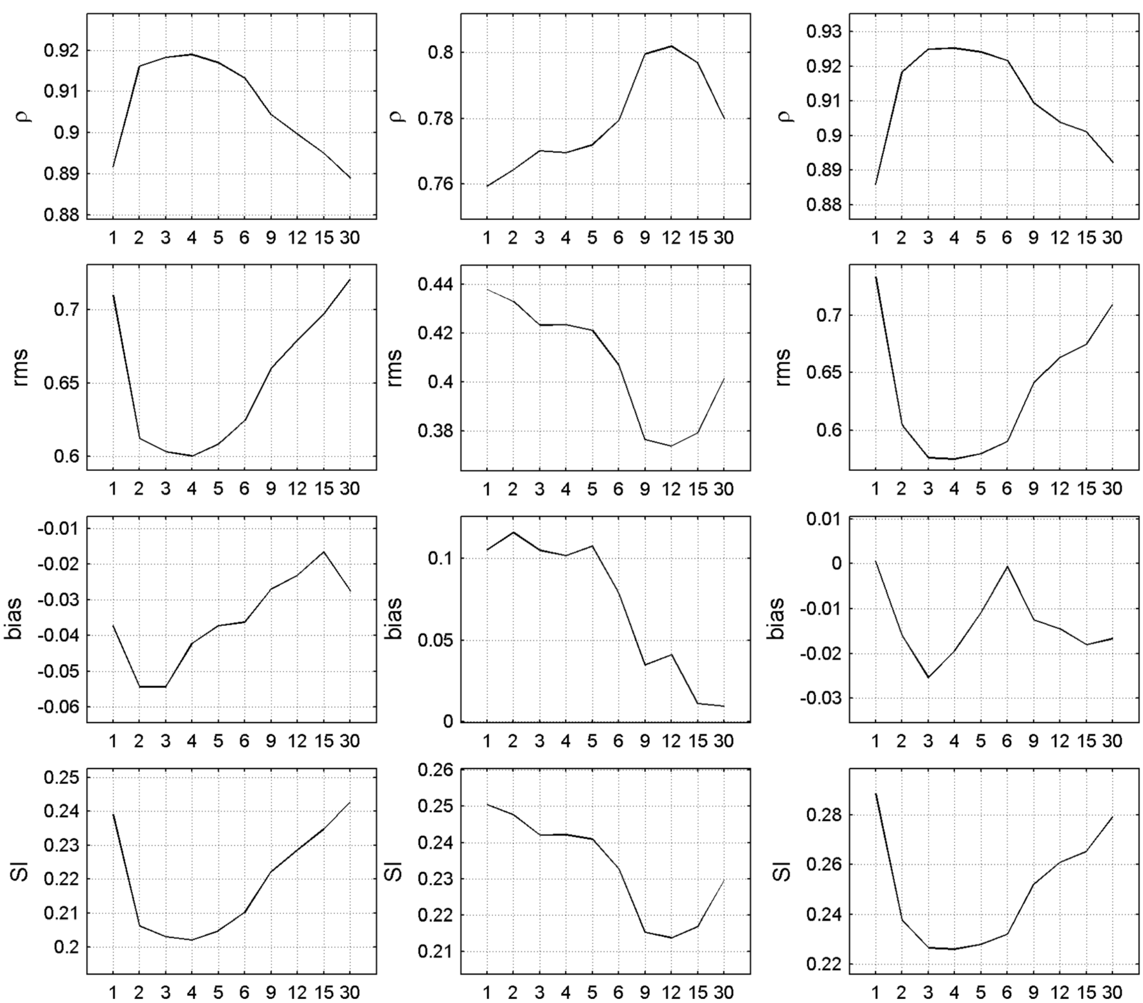

Fig. 4 Sensitivity analysis of the multivariate regression model of the daily significant wave height using a regional predictor with different temporal coverages (in days) at three different locations: Spanish northwest coast (*left panels*); Peruvian location (*middle panels*); Oregon location (*right panels*). Correlation coefficient (ρ), root mean square error (*rms*), bias, scatter index (*SI*)

N being the dimension of the original data. In this study, $N = 2N1 + 2N2$, $N1$ being the number of source points in the regional area (345 grid points) and $N2$ the number of source points in the local area (35 grid points). The number of grid points of the regional and local areas are multiple by 2 because the predictor is defined by means of the SLP fields and squared SLP gradient fields. The EOFs are ranked in an increase order of explained variance. A dimension reduction can be obtained while keeping a high amount of variance. In this study, a variance equal to 95 % is considered. Therefore, the daily predictor can be defined by the principal components at a daily scale:

$$X(x, t_i) = EOF_1(x) \times PC_1(t_i) + EOF_2(x) \times PC_2(t_i) + \ldots + EOF_d(x) \times PC_d(t_i) \quad (2)$$

where d=41 is the number of EOFs explaining the 95 % variance of the original data.

Figure 3 shows the first six EOFs with the target location and its corresponding PCs of the predictor, with the PCs being standardized and the EOFs multiplied by the corresponding standard deviation. EOF1 explains 28.58 % of the variance; EOF2, 18.78 %; EOF3, 10. 36 %; EOF4, 5.62 %; EOF5, 5.04 %; and EOF6, 3.83 %. The variability spatial patterns are defined by the anomalies of SLP and squared SLP gradients in the generation and local areas. The SLP anomalies are represented by contour lines, plotting the positive anomalies in red and the negative in blue. The anomalies of the squared SLP gradients are represented in a blue-white-red scale. Note that the land points are not considered in the predictor definition. In this case, noise in the predictor of wave climate due to a strong gradient in Greenland which would determine the variability pattern identification is avoided.

3.3 Optimal historical temporal coverage of the regional predictor

The optimal historical temporal coverage (n-days) of the regional predictor is defined in this step of the method. A multivariate regression model between the daily significant wave height at the target location (predictand) and the corresponding daily PCs (predictor) is applied considering several temporal coverages. Data from 1960 to 1999 define the calibration period of the statistical model. Data from 2000 to 2008 are used as a model validation period. The number of predictor PCs

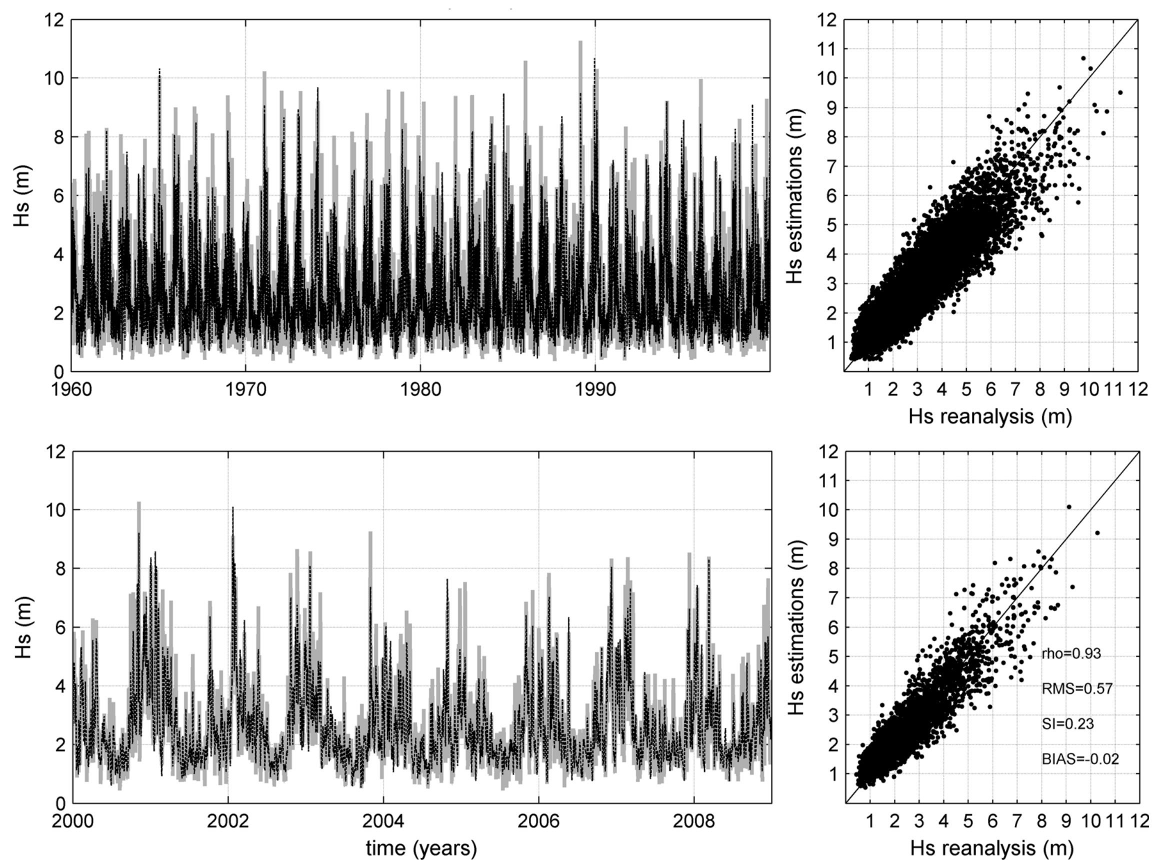

Fig. 5 Multivariate regression model of the daily significant wave height at the Spanish northwest coast using a regional predictor with a historical temporal coverage of 4 days. *Upper panel*: calibration period. *Lower panel*: validation period

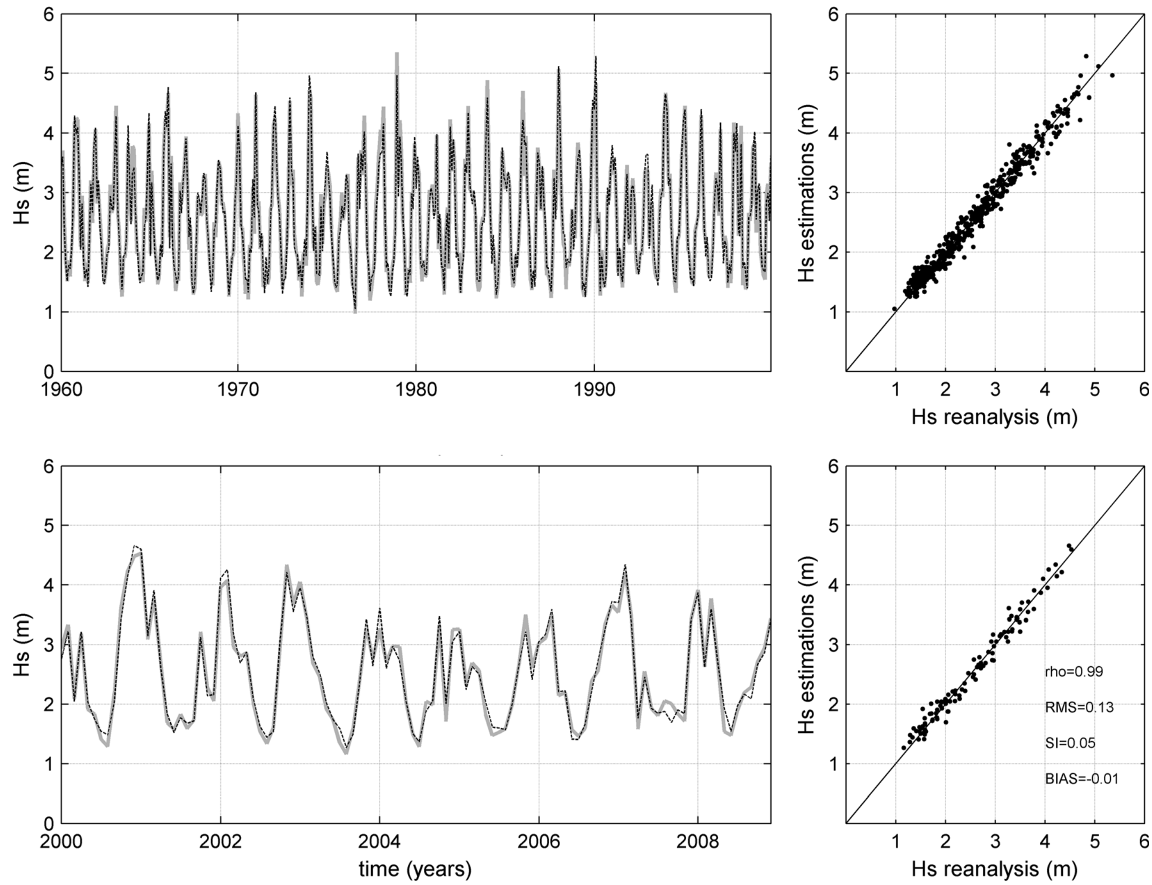

Fig. 6 Multivariate regression model of the monthly significant wave height at the Spanish northwest coast using a regional predictor with a historical temporal coverage of 4 days. *Upper panel*: calibration period. *Lower panel*: validation period

are selected in a forward procedure. The first predictor is obtained from the best fit (smallest sum of squared error, SSE) among all the d model fits with a single predictor (d being the number of all potential predictors, in this case, PC_i, $i=1, \ldots, d$). The second predictor is chosen from the rest of the predictors (d-1, except the one selected previously) from the best fit among d-1 model fits with two predictors, the best predictor selected in the previous model plus one of the remaining potential predictors. The cycle continues until a more complicated model does not produce a significant improvement (at the 5 % level of significance) to the multivariate regression fit. This evaluation is based on the F statistics that compare the SSE of the fit of a simpler-parameter model with that of a more complicate parameter model (see Wang et al. 2004 for details).

The multivariate regression model is fitted for different historical temporal coverages of the regional predictor at the northwest Spanish location. Several indicators of the quality of the fittings in the validation period are calculated in order to select the optimum temporal coverage of the regional predictor. The skill indicators are the correlation coefficient (ρ), the root mean square error (rms), the bias (bias), and the scatter index (SI). Figure 4 shows the values of these indicators for different n-days for the regional predictor (1, 2, 3, 4, 5, 6, 9, 15, and 30 days). The results presented in the left panels correspond to the Spanish location. It can be observed that the best statistical model is obtained using a predictor with a temporal coverage of 4 days (n=4). The calibration of the multivariate regression model at daily scale at the northwest Spanish location, using a regional predictor with a temporal coverage of n=4 days, is shown in the upper panel of Fig. 5. The validation of

Table 1 Monthly PCs selected by the regression model

PC	1	6	3	5	11	4	24	9	15	13
bi	−0.8434	0.2717	−0.2531	0.1844	−0.0538	−0.0650	−0.0660	−0.0380	−0.0476	0.0516
PC	2	16	8	31	30	20	21	27	19	18
bi	0.0312	−0.0409	0.0325	−0.0227	−0.0258	−0.0283	−0.0242	−0.0232	−0.0249	−0.0175

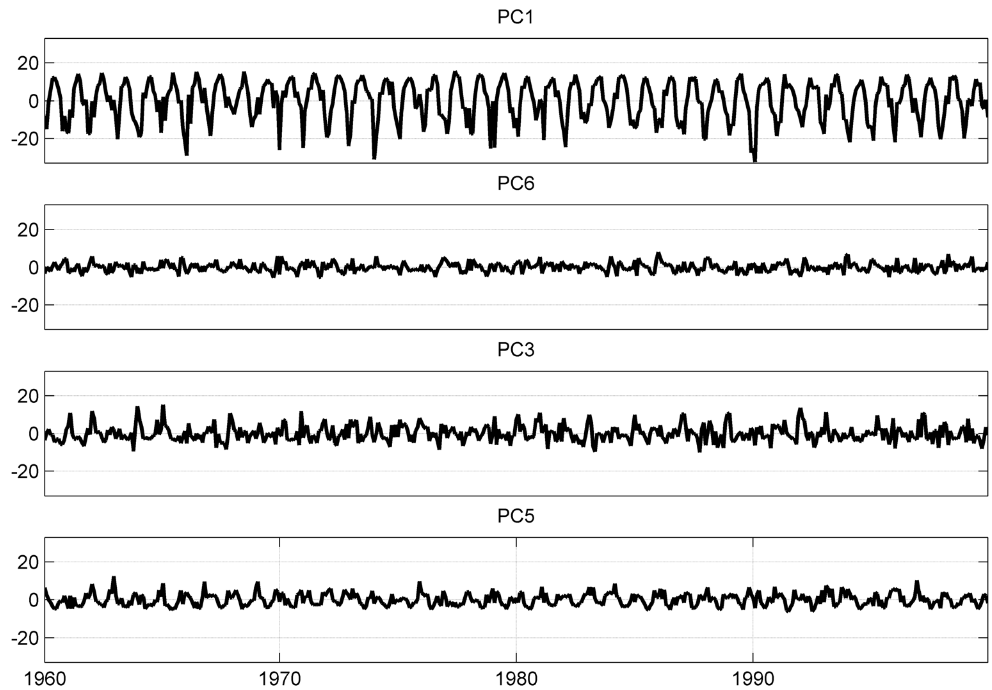

Fig. 7 Monthly wave predictor indices for the Spanish northwest location using the proposed method

the model is shown in the lower panel, where the capability of the model to reproduce the daily significant wave height can be observed.

3.4 Monthly wave predictor indices

The monthly values of the principal components (PCi_m), with a historical temporal coverage of the regional predictor equal to 4 days, are used as the potential monthly wave predictor indices for the Spanish location. The calibration and validation of the multivariate regression model at monthly scale is shown in Fig. 6. As it can be seen, the seasonal and interannual variability of the monthly wave height is well represented.

The statistical model is defined as a linear combination of the most important monthly PCs of the predictor defined specifically for the analyzed target location (PCi_m), selected in a forward procedure:

$$Y_m(t) = 2.8254 - 0.8434 \times \mathrm{PC1}_m(t) + 0.2717 \times \mathrm{PC6}_m(t) - 0.2531 \times \mathrm{PC3}_m(t) + 0.1844 \times \mathrm{PC5}_m(t) + \ldots$$

The total monthly PCs selected by the multivariate model with their corresponding coefficient are detailed in Table 1.

The most important predictor is the $\mathrm{PC1_m}$, followed by the $\mathrm{PC6_m}$, $\mathrm{PC3_m}$, and $\mathrm{PC5_m}$ (see Fig. 7). Therefore, these predictors define the monthly wave predictor indices for that specific location. The monthly significant wave height is slightly better reproduced using the monthly values of the principal components from the daily predictor (ρ=0.99, rms=0.1316, bias=−0. 0092, si=0.0517), compared to using monthly SLP and monthly squared SLP gradients (ρ=0.98, rms=0.1740, bias=−0. 164, si=0.0684).

Besides the improvement of the downscaling statistical model of the monthly significant wave height, the defined wave predictor indices can be used to provide additional info of the local wave climate. The analysis of the directional spectrum helps to understand the effect of remote winds, besides local winds, responsible for wave generation at a target location (Espejo et al. 2014). Therefore, hourly wave spectra from the GOW database at the northwest Spanish location are used to explore the wave climate variability by

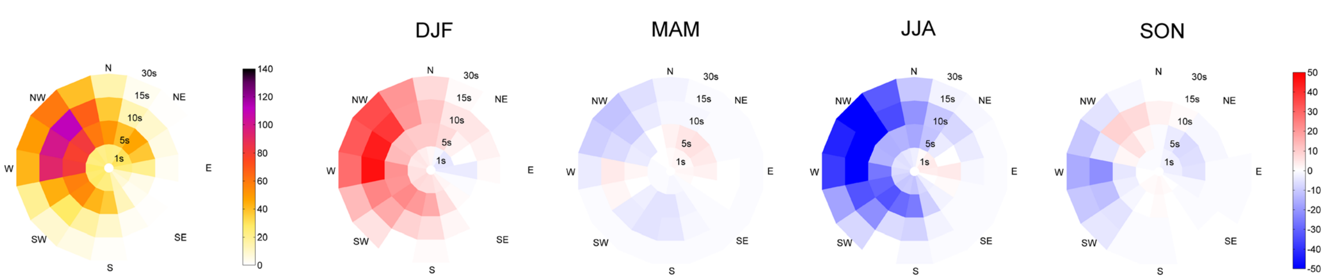

Fig. 8 Spectral wave climate at the Spanish northwest location: mean spectrum and seasonal spectral anomalies

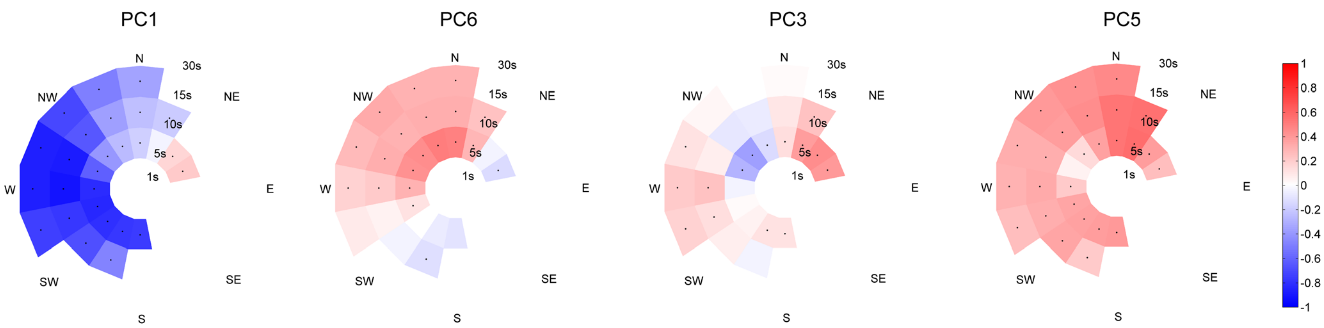

Fig. 9 Correlation between the monthly wave energy spectrum and the first four monthly wave predictor indices obtained with the proposed method ($PC1_m$, $PC6_m$, $PC3_m$, $PC5_m$)

means of the correlation with the monthly wave predictor indices obtained. Figure 8 represents the mean annual wave spectrum at the target location and the corresponding seasonal anomalies. There is a clear energy peak on the WNW sector and periods between 10 and 15 s. This peak is enhanced during winters, while the anomalies are negative during summers, reflecting the seasonal fluctuation of the atmospheric circulation in the North Atlantic. Negative NW anomalies and small positive NE anomalies on the short periods are also found at spring, in line with Espejo et al. (2014) using instrumental data from Villano buoy.

Figure 9 shows the correlation of the monthly wave energy spectra (the bin energy associated to each sector and period range) with the first four monthly wave climate indices ($PC1_m$, $PC6_m$, $PC3_m$, $PC5_m$). The bin is dotted when the correlation is significant at 90 % confidence. The $PC1_m$ presents the highest correlation with the monthly wave spectra. The negative phase of the corresponding EOF1 (see the upper left panel of Fig. 3), characterized by low pressure center located in the middle of North Atlantic Ocean, correlates positively with the energy contained in all the period bands of the SW and NW directional sector. The $PC1_m$ seasonal component agrees with the seasonal fluctuation of wave energy spectra. In the case of the $PC3_m$, its EOF3 reflects a more local variability pattern (see the middle left panel of Fig. 3). The EOF3-positive phase is characterized by a high pressure center in the north of Spain, generating local winds from the NE direction, and a low pressure center in the southwest part of the North Atlantic, causing winds from the SW. Thus, the positive phase of this variability pattern enhances wave energy from the NE and from the SW, reflected in the positive correlation with these corresponding wave energy spectrum bins (shorter period in the case of the NE wave energy). The EOF3-negative phase is defined by a high pressure center in the north of Spain. Winds from the NW direction generated an increase of wave energy from that sector, corresponding to a

Fig. 10 Correlation between the monthly wave energy spectrum and the $PC2_m$ wave climate index (*upper left panel*) or NAO index (*upper right panel*). Correlation between $PC2_m$ and the NAO index (*lower panel*)

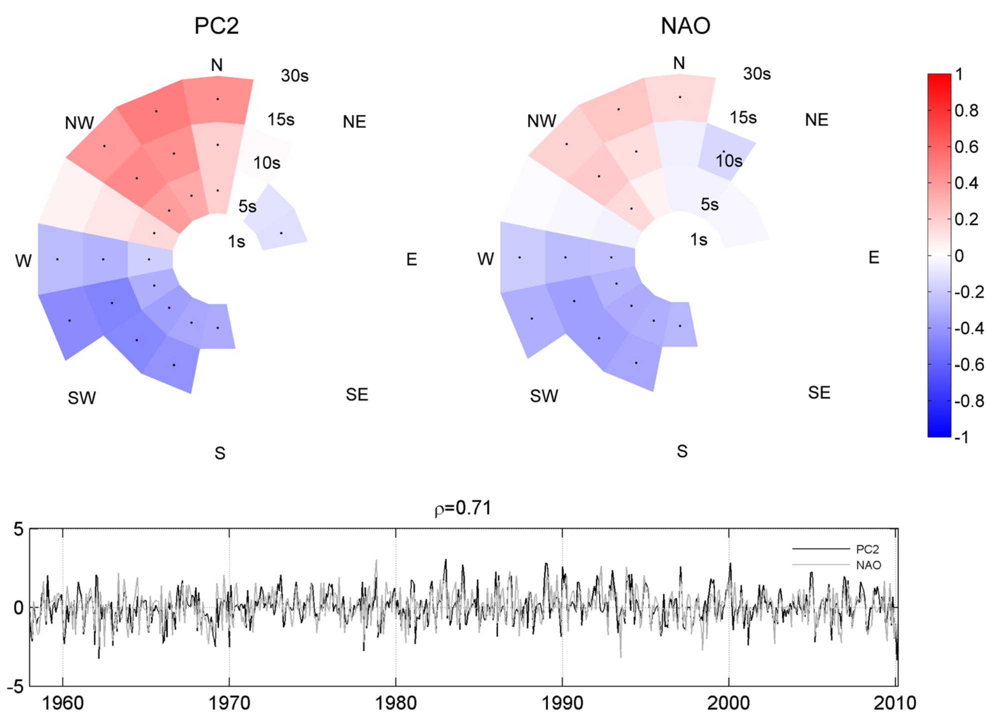

negative correlation with $PC3_m$. The physical interpretation of the correlation of $PC6_m$ and $PC5_m$ is not so obvious due to a more complicated spatial structure of the variability patterns.

The comparison of the correlation between the monthly wave energy spectrum and the $PC2_m$ wave climate index (upper left panel) or NAO index (upper right panel) is represented in Fig. 10. The correlation between $PC2_m$ and the NAO index is shown in the lower panel. A correlation coefficient around 0.7 is obtained. The EOF2 variability pattern resembles the NAO pattern (see the right upper panel of the Fig. 3), characterized by a pressure dipole centered close to Iceland and Azores. However, the correlation of the wave energy spectra with $PC2_m$ is higher than with NAO because EOF2 is a variability pattern particularly obtained for the northwest Spanish location. The EOF2-positive phase, characterized by low pressure center at Iceland and high pressure center at Azores, presents a positive correlation with wave energy from the NW sector and a negative correlation with wave energy from the SW.

4 Other applications

The proposed method is applied in two other locations with different wave climate: Trujillo (Perú) [80° W, 8° S] and Oregon (USA) [131° W, 46° N].

The ESTELA method is used to determinate the local and generation area of the predictor for waves at Trujillo location. The effective energy flux of the source points and the gain/loss energy map inform that wave energy coming from both hemispheres is arriving at the target location (see Figure 8 of Perez et al. 2014, in this issue). The predictor area of influence considered covers almost the whole Pacific Ocean. The left panels of Fig. 11 show the first and the fourth spatial variability patterns (EOFs) of the daily predictor (the local predictor area is delimited by a black box). The optimum historical temporal coverage is established in 12 days (see the panels of the middle column of Fig. 4). The validation of the statistical model relating significant wave height

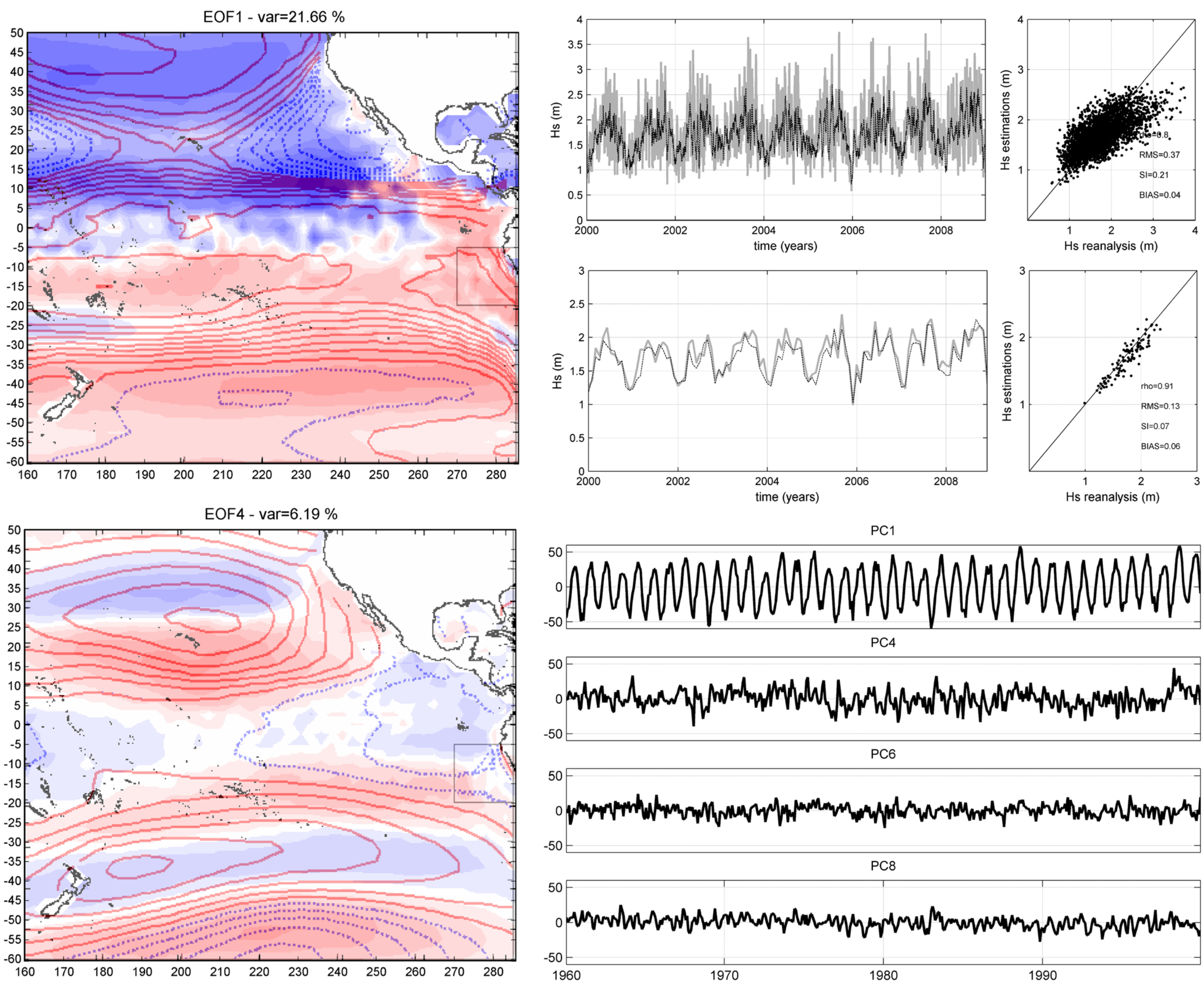

Fig. 11 Spatial patterns of daily predictor for temporal coverage of 12 days for the regional predictor for the Peruvian location (*left panels*). Validation of the statistical model at daily and monthly scales (*upper right panels*). Monthly wave predictors (*lower right panel*)

and wave predictor indices are represented in the upper right panels of Fig. 11, at daily and monthly scale, respectively. The good model fitting can be observed. The first four PCs selected by the statistical model, which are the local monthly wave predictor indices for Trujillo, are represented in the lower right panels of Fig. 11. The model fit using monthly values of the PCs of the daily predictor with a temporal coverage of 12 days for the regional component is slightly better (ρ=0.9139, rms=0.1385, bias=0.0718, si=0.0793) than the model fit using the PCs of the monthly SLP and squared SLP gradients (ρ=0.8991, rms=0.1316, bias=−0. 0092, si=0.0517).

In the case of Oregon location, an optimum historical temporal coverage of 4 days is selected (see the panels of the right column of Fig. 4). The regional predictor area, obtained using ESTELA method, covers only the north hemisphere of the Pacific Ocean (see Figure 5 of Perez et al. 2014, in this issue). The upper right panels of Fig. 12 show the validation of the multivariate regression model for an optimum historical temporal coverage of 4 days at Oregon location. A good performance of the model is obtained using the daily or monthly values of the temporal coefficients of the predictor variability modes. The first four local monthly wave predictor indices for the Oregon location are represented in the lower right panel of Fig. 12. The corresponding EOFs of the daily predictor are represented in the left panels of Fig. 12. The spatial domain of the local predictor is marked.

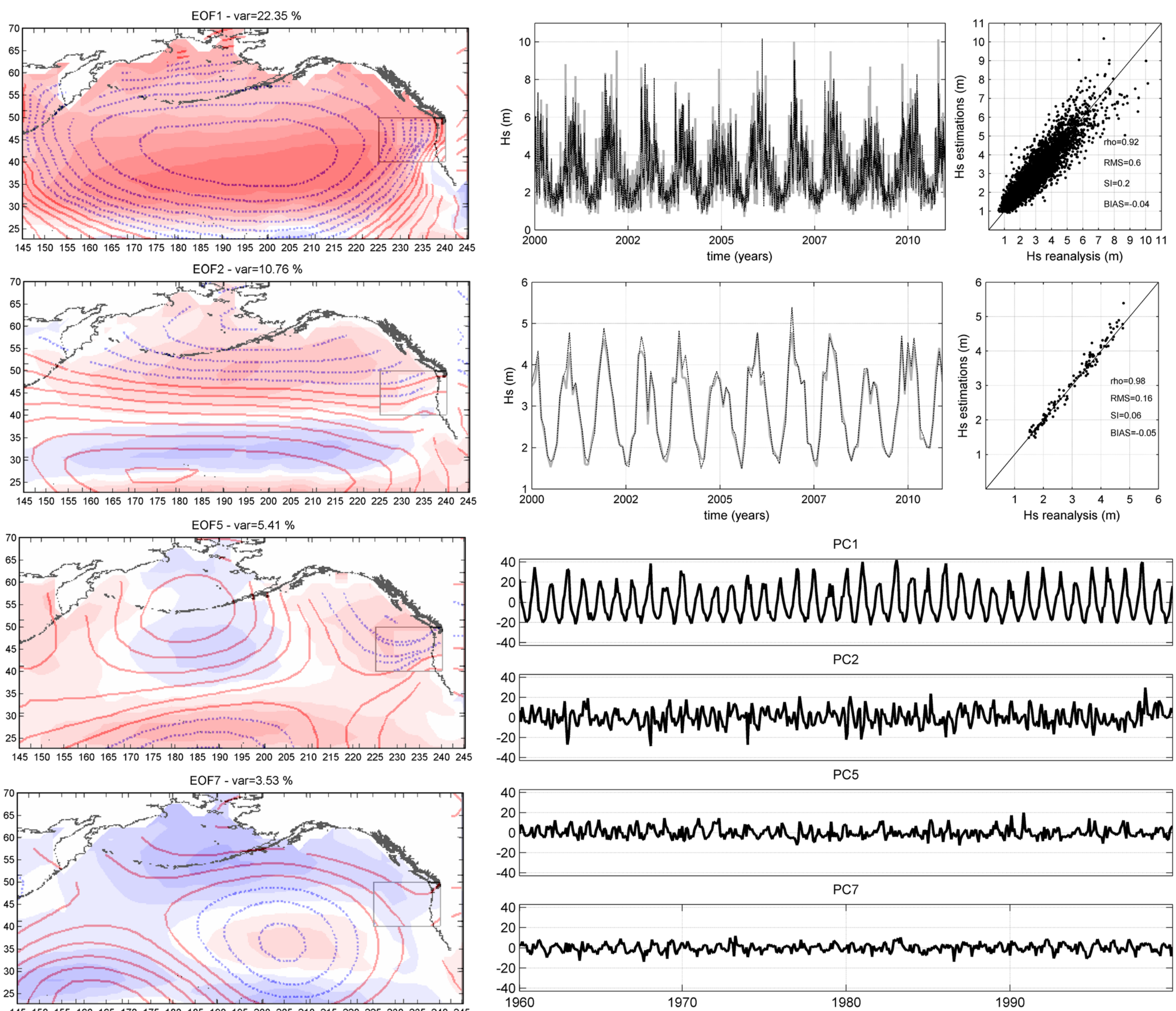

Fig. 12 Spatial patterns of daily predictor for temporal coverage of 4 days for the regional predictor for Oregon location (*left panels*). Validation of the statistical model at daily and monthly scales (*upper right panels*). Monthly wave predictors (*lower right panel*)

5 Summary and conclusions

A method to obtain local monthly wave predictor indices has been proposed. The method is based on the statistical relationship between the atmospheric predictor, characterized by the SLP and the squared SLP gradient fields, and the local wave climate.

The spatial domain and the temporal coverage are the key properties of the wave predictor. The predictor is composed of a regional predictor, representative of the swell wave component, and a local predictor, representative of the sea component. The ESTELA method (Perez et al. 2014, this issue) has been implemented to characterize the footprint of the wave climate at a specific location of interest and to automate the definition of the spatial domain of the predictor corresponding to the swell wave component. The ESTELA map also helps to determinate the predictor local area, extended to the 1-day energy flux travel time line. A global historical temporal coverage for the regional predictor is required to represent the recent history of atmospheric conditions responsible for the swell wave component of the wave climate at the target location. Both predictor components with different spatial domain and temporal resolution are joined at a daily scale. PCA is applied to identify the main variability patterns particularized to the target location. Different *n*-days are considered in order to obtain the best representative temporal coverage of the regional predictor. The optimal historical temporal coverage of the regional predictor is obtained associated to the best solution of a multivariate regression model, between the daily significant wave height and the principal components of the daily predictor. The multivariate regression is fitted using a forward selection procedure in order to guarantee the most important predictor PCs.

The monthly wave climate conditions are modeled applying a multivariate regression model using the monthly values of the principal components of the daily predictor, with the optimum historical temporal coverage for the regional predictor. The selected monthly PCs for the optimum temporal coverage are the monthly wave predictor indices for the target location. The local monthly indices identified with this method improve the statistical model fitting of the monthly mean significant wave height, compared with a predictor defined as the corresponding monthly SLP and squared SLP gradients at a regional scale. A stronger relation with the local wave climate is obtained with these monthly indices, resulting in a higher correlation with wave spectra. The variability patterns associated with the indices allow a better understanding of the origin of the complex wave fields.

We believe that the outcomes of this work can contribute to improve the predictions of wave climate at daily and monthly scales. In particular, the daily predictor can be applied in wave climate projections for different CMIP5 based on statistical downscaling (Wang et al. 2014), and the monthly predictor could help to explain long-term morphodynamic anomalies (Barnard et al. 2011). This statistical downscaling approach can be used in extratropical areas. Further research is needed to extend this method to tropical regions affected by tropical cyclones.

Acknowledgments The work was partly funded by the project iMar21 (CTM2010-15009) from the Spanish Government and the FP7 European projects CoCoNet (287844) and Mermaid (288710). The authors would like to thank the anonymous reviewers for their valuable comments and suggestions to improve the quality of the paper.

References

Barnard PL, Allan J, Hansen JE, Kaminsky GM, Ruggiero P, Doria A (2011) The impact of the 2009–10 El Niño Modoki on U.S. West Coast beaches. Geophys Res Lett 38((13):L13604

Caires S, Swail VL, Wang XL (2006) Projection and analysis of extreme wave climate. J Clim 19:5581–5605

Casas-Prat M, Wang XL, Sierra JP (2014) A physical-based statistical method for modeling ocean wave heights. Ocean Model 73:59–75

Dodet G, Bertin X, Taborda R (2010) Wave climate variability in the North-East Atlantic Ocean over the last six decades. Ocean Model 31(3–4):120–131

Espejo A, Camus P, Losada,I, Mendez F (2014) Spectral ocean wave climate variability based on atmospheric circulation patterns. J Phys Oceanogr. doi:10.1175/JPO-D-13-0276.1

Fan Y, Lin S-J, Held IM, Yu Z, Tolman HL (2012) Global ocean surface wave simulation using a coupled atmosphere-wave model. J Clim 25:6233–6251

Gulev SK, Grigorieva V (2006) Variability of the winter wind waves and swell in the North Atlantic and North Pacific as revealed by the voluntary observing ship data. J Clim 19:5667–5685

Hemer M (2010) Historical trends in Southern Ocean storminess: long-term variability of extreme wave heights at Cape Sorell, Tasmania. Geophys Res Lett 37, L18601

Hemer MA, Church JA, Hunter JR (2010) Variability and trends in the directional wave climate of the Southern Hemisphere. Int J Climatol 30(4):475–491

Hurrell JW (1995) Decadal trends in the North Atlantic Oscillation: regional temperatures and precipitation. Science 269:676–679

Izaguirre C, Méndez FJ, Menéndez M, Luceño A, Losada IJ (2010) Extreme wave climate variability in southern Europe using satellite data. J Geophys Res 115, C04009 J

Izaguirre C, Méndez FJ, Menéndez M, Losada IJ (2011) Global extreme wave height variability based on satellite data. Geophys Res Lett 38, L10607

Kalnay EM, Kanamitsu R, Kistler W, Collins D, Deaven L, Gandin M, Iredell S, Saha G, White J, Woollen Y, Zhu M, Chelliah W, Ebisuzaki W, Higgins J, Janowiak KC, Mo C, Ropelewski J, Wang A, Leetmaa R, Reynolds R, Jenne R, Joseph D (1996) The NCEP/NCAR 40-year reanalysis project. Bull Am Meteorol Soc 77: 437–470

Mínguez R, Espejo A, Tomás A, Méndez FJ, Losada IJ (2011) Directional calibration of wave reanalysis databases using instrumental data. J Atmos Ocean Technol 28(1):1466–1485

Mínguez R, Reguero BG, Luceño A, Méndez FJ (2012) Regression models for outlier identification (hurricanes and typhoons) in wave hindcast databases. J Atmos Ocean Technol 29(2):267–285

Noaa NGDC (2006) Etopo2v2 global gridded 2-minute database

Perez J, Menéndez M, Méndez FJ, Losada IJ (2014) ESTELA: A method for evaluating the source and travel-time of the wave energy reaching a local area. Submitted to the 13th Wave Topical Collection of Ocean Dynamics

Rascle N, Ardhuin F (2012) A global wave parameter database for geophysical applications. Part 2: model validation with improved source term parameterization. Ocean Model. doi:10.1016/j.ocemod.2012.12.001

Rascle N, Ardhuin F, Queffeulou P, Croizé-Fillon D (2008) A global wave parameter database for geophysical applications. Part 1: wave-current-turbulence interaction parameters for the open ocean based on traditional parameterizations. Ocean Model 25(3–4):154–171. doi:10.1016/j.ocemod.2008.07.006

Reguero BG, Menéndez M, Méndez FJ, Mínguez R, Losada IJ (2012) A Global Ocean Wave (GOW) calibrated reanalysis from 1948 onwards. Coast Eng 65:38–55

Ropelewski CF, Jones PD (1987) An extension of the Tahiti-Darwin Southern Oscillation index. Mon Weather Rev 115:2161–2165

Semedo A, Sušelj K, Rutgersson A, Sterl A (2011) A global view on the wind sea and swell climate and variability from ERA-40. J Clim 24: 1461–1479

Sterl A, Caires S (2005) Climatology, variability and extrema of ocean waves: the web-based KNMI/ERA-40 wave atlas. Int J Climatol 25(22):963–977

Stopa JE, Cheung KF, Tolman HL, Chawla A (2012) Patterns and cycles in the climate forecast system reanalysis wind and wave data. Ocean Model 70:207–220

Thompson DWJ, Wallace JM (1998) The Arctic Oscillation signature in the wintertime geopotential height and temperature fields. Geophys Res Lett 25(5):1297–1300

Tolman HL (2002) User manual and system documentation of WAVEWATCH III version 2.22. NOAA/NWS/NCEP Technical Note

Trenberth KE, Hurrell JW (1994) Decadal atmosphere-ocean variations in the Pacific. Clim Dyn 9:303–319

Walker GT, Bliss EW (1932) World weather V. Mem R Meteorol Soc 4(36):53–83

Wang XL, Swail VR (2006) Climate change signal and uncertainty in projections of ocean wave heights. Clim Dyn 26:109–126

Wang XL, Zwiers FW, Swail VR (2004) North Atlantic Ocean wave climate change scenarios for the twenty-first century. J Clim 17: 2368–2383

Wang XL, Feng Y, Swail VR (2012) North Atlantic wave height trends as reconstructed from the 20th century reanalysis. Geophys Res Lett 39, L18705

Wang XL, Feng Y, Swail VR (2014) Changes in global ocean wave heights as projected using multimodel CMIP5 simulations. Geophys Res Lett 41(3):1026–1034

Woolf DK, Challenor PG, Cotton PD (2002) Variability and predictability of the North Atlantic wave climate. J Geophys Res 107(C10):3145